

Rearranged gene order between pig and human in a QTL region on SSC 7

Olivier Demeure,¹ Christine Renard,² Martine Yerle,¹ Thomas Faraut,¹ Juliette Riquet,¹ Annie Robic,¹ Thomas Schiex,³ Anette Rink,⁴ Denis Milan¹

¹Laboratoire de Génétique Cellulaire, INRA, BP 27, 31326 Castanet-Tolosan, France

²Laboratoire de Radiobiologie et d'Etude du Génome, INRA, 78352, Jouy En Josas, France

³Station de Biométrie et d'Intelligence Artificielle, INRA, BP 27, 31326 Castanet-Tolosan, France

⁴Department of Animal Biotechnology, University of Nevada, Reno, Nevada 89557, USA

Received: 21 May 2002 / Accepted: 17 September 2002

Abstract

On porcine Chromosome 7, the region surrounding the MHC region contains QTL influencing many traits including growth, back fat thickness, and carcass composition. Towards the identification of the responsible gene(s), this article describes an increase of density of the radiated hybrid map of SSC 7 in the q11-q14 region and the comparative analysis of gene order on the porcine RH map and human genome assembly. Adding 24 new genes in this region, we were able to build a framework map that fills in gaps on the previous maps. The new software Carthagene was used to build a robust framework in this region. Comparative analysis of human and porcine maps revealed a global conservation of gene order and of distances between genes. A rearranged fragment of around 3.7 Mb was, however, found in the pig approximately 20 Mb upstream from the expected location on the basis of the human map. This rearrangement, found by RH mapping on the IMpRH 7.000 rads panel, has been confirmed by two-color FISH and by mapping on the high resolution IM-NpRH2 12.000 rads panel. The rearranged fragment contains two microsatellites found at the most likely QTL location in the INRA QTL experiment. It also contains the *BMP5* gene, which, together with *CLPS*, could be considered as a possible candidate.

Introduction

In different studies, swine Chromosome 7 (SSC 7) has been shown to be rich in QTL affecting economical and quality traits such as growth, back fat

thickness, and carcass composition (de Koning et al. 1999, 2001; Bidanel et al. 2001; Malek et al. 2001; Milan et al. 2002). First analyses mapped those QTL close to the Major Histocompatibility Complex (MHC), also called Swine Leukocyte Antigens (*SLA*), with a most likely position in the SSC 7p12-q12 region (Bidanel et al. 2001). In pigs, *SLA* is split in two parts by the centromere; the MHC class I and III are located on the p arm, while class II is on the q arm (Chardon et al. 2000). An important step towards the identification of the responsible gene(s) is to better characterize the chromosomal region where QTL are localized, and in particular to identify genes located in this area. To determine gene order in mammalian species, RH mapping has become the tool of choice (Cox et al. 1990; Walter et al. 1994; Robic et al. 1999; Gu et al. 1999; Amarante et al. 2000). For the pig genome, a 7000-rad IMpRH radiation hybrid panel has been developed at INRA (Yerle et al. 1998) and has been characterized at the University of Minnesota (Hawken et al. 1999). Previously we demonstrated that genes located close to the *SLA* complex on the p arm of SSC7 are largely found in the same order as on HSA 6p (Genet et al. 2001). However, if the QTL region includes the *SLA* complex, it seems that the most likely region is lying between the *SLA* and marker *S0102* at the top of the q arm of SSC 7 (Bidanel et al. 2001; Milan et al. 2002). As only the *colipase* gene was mapped in the porcine region in correspondence with HSA 6p12-p21 (Genet et al. 2001), development of a map at a higher density was required in this region.

In the past years, very few porcine sequences were available. To develop a marker for new genes in the pig, it was thus necessary to align sequences available in various species (human, mouse, rat...) and to develop primers in conserved regions. Re-

Correspondence to: D. Milan; E-mail: milan@toulouse.inra.fr

Table 1. Primer sequences and PCR conditions for the 24 markers mapped on RH panels. The primer selection strategy is represented by a) 3' UTR, b) microsatellite, c) framing one intron, d) into an exon, e) 5' UTR.

Marker	GenBank ID	Primer Sequences	Annealing T°	MgCl ₂ (mM)	Primers (μM)	Size of fragment (bp)	Retention frequency on IMPRH7.000
BAG2 a	NM 004282	CGC CTG TTC TTC CGA GGT GCA TTT CTA CGC CAT TAT TTC AAG	58	1.5	0.5	255	49
BMP5 b	microsatellite	TTT CGA AAG AGA CTA AAA CCAT CC AGG CAC AGA GAA GGA CTG GA	58	1.5	0.5	197	50
BYSL c	NM 004053	CCA CCT CTA CAT GGC ACT CAA GAT GAT GGC TTC CCG GAG	58	1.5	0.5	±200	28
CD2AP a	NM 012120	TGA TAG ACT AAC GGG TGG AGA ATG GAA GCA TGA TAG CTG GT	58	1.5	0.25	315	22
DAXX b	microsatellite	GTG TCA GCA GGC AGG AAG A GTG GCA TAG GTT GGT GGC	55	1.5	0.5	191	39
DEF6 c	NM 022047	AGG CCA GTA CCA ATG TGA AA TTC TGC TGC TCA CTG CTG	58	1.5	0.5	±300	41
DKFZP566C243 c	NM 015388	ATC TGC ATT TCG CCT ACC AC ACA GAT TTC AGG TGG GGT CA	55	1.5	0.5	±300	22
ENPP4 d	NM 014936	TAT GCT GCT GTG CTT TCT GG TCC ATC TCA TCT TTG TCC TTC A	58	1.5	0.25	464	22
FLJ10775 e	NM 018214	GGG ATG CTG AAT GTG GTA TTT TTT TCT CTT TTT GTG CTT TTC TG	58	3	0.25	287	50
FLJ13159 d	NM 021940	TGT GCT GTT GTT ATG ATG TGC T TGA AGT GGC TTG TTT AGT TAC CC	58	1.5	0.5	217	33
FLJ13222 a	NM 021943	CGA ATG ACA CCC ACC TTT TC GTT CCC CAG CAC CTC TGT T	58	3	0.25	237	32
FLJ20337 c	NM 017772	CTG TGA CCC TCC CTC GAC T TCC ACA ATT TCC CAT ACA AAC A	55	1.5	0.5	±100	34
GLO1 a	NM 006708	TTT CCC TTT CCC ATT TTA GC GGA GAA AGA AAG CAA ATG CAG	55	3	0.25	164	41
GNMT c	NM 018960	CGA CAT CTG TGC TGA CAG TG TGG ATG AAA TAG CAG GGA ATG	58	1.5	0.5	±350	30
HELO1 a	AL 136939	CAT CAA GGG CAA AGA ATG TT CAC AAG ACT ACT TAA GAG AAC CAA CT	58	3	0.5	173	23
HKE4 c	NM 006979	CCG CTC TCT GCT CCA GAT AAG AAA GGC GAC AAT TCC AC	58	1.5	0.5	±500	54
HRHFB2436 c	NM 014345	GGT GCC CAG ATG ACC CAG GGT GAG CCA GAT AGA CAT TTT GAT T	58	1.5	0.5	±250	27
LOC51323 d	NM 016629	GCT GAT TGT ATG GTT TTT CAC CT AAT GGG AGC AGA GTT GTT GC	58	1.5	0.25	437	25
MCM3 c	NM 002388	TCC GAA TGC ACC GCT ACC TGC TGG TCT TCC TGG CTA AAG T	58	1.5	0.5	±500	19
NFYA b	microsatellite	TTG GGT TTC TGA GCC TTA GC TGT GGC TCC TAA CCC AAA GT	58	1.5	0.5	211	34
PTK7 c	NM 002821	CCT GGA GGG CGA CTT CTC ATC AGC CGG TAG AGC TTG G	58	1.5	0.5	±1000	30
RAB2L c	NM 004761	AAG TGT CAT CAN GTC GTG TCC	58	1.5	0.5	±300	42

Continued on next page

Table 1. Continued

Marker	Genbank ID	Primer Sequences	Annealing T°	MgCl ₂ (mM)	Primers (µM)	Size of fragment (bp)	Retention frequency on ImpRH7.000
TNX b	microsatellite	GCC CAG CCGT AGC AGT AGA G GTT GGA GGT GAG GGA AGA TT	58	1.5	0.5	194	39
WAFI b	microsatellite	TGT GGA TTT TTC ATA CAT GTG AGT ACG GCA ACC CCA CTT TGT GCC TAC TGT CCC TTC CAC CT	60	1.5	0.5	297	28
ZNF76 c	NM 003427	GCA TCC CTT CAT CAT CAA CA TGA TGG CCT CCT CTA AGG TC	58	1.5	0.5	±1000	36

cently, numerous ESTs were made available in pigs (Fahrenkrug et al. 2000; Rink et al. 2002), which allow primer design based on pig sequence directly. To take advantage of the availability of these sequences, the ICCARE (Interspecific Comparative Clustering and Annotation for Ests) tool was developed to systematically compare porcine ESTs relative to sequence of human genes, and to display an ordered list of porcine ESTs homologous to genes selected on a human chromosome (Faraut et al. in preparation). For a given gene of interest, all available porcine ESTs and sequences are aligned with human sequence. This facilitates the design of primers on annotated porcine sequences, taking into account the exon-intron organization, extrapolated from information available from human genomic sequence. Primers were designed for 20 genes by using ICCARE. Additionally, we mapped five microsatellite markers developed from BACs screened with known genes in a project of contig development in the region surrounding the *SLA* complex (Barbosa et al. in preparation). Subsequently, 25 genes located in humans between HSA 6p21.3 and HSA 6q12-q13 (from *TNX* to *FLJ13159*) were mapped.

Materials and methods

Markers. ICCARE allowed us to select 28 genes in the region between *RXRβ* and *FLJ13159* for which a porcine sequence is available (see Table 1). We also selected five microsatellites subcloned from BACs known to contain a gene close to the *SLA* region. Primers were designed using Primer3 (http://www-genome.wi.mit.edu/cgi-bin/primer/primer3_www.cgi).

PCR amplification and radiation hybrid mapping. Amplifications were carried out on a GeneAmp System 9700 (Applied Biosystem, Courtaboeuf, France) thermocycler. Reactions were performed in duplicate on IMpRH (7000 Rads) or IMNpRH2 (12000 Rads) panels. Thermal cycling parameters were denaturation at 95°C for 5 min, followed by 30 cycles of 95°C for 30 s/annealing temperature for 30 s/72°C for 45 s; a final amplification was performed at 72°C for 15 min. PCR products were analyzed on a 2% agarose gel, electrophoresed in 1 × TBE buffer, and visualized by ethidium bromide staining.

Map construction. Vectors were submitted to IMpRH Server at <http://imprh.toulouse.inra.fr/> (Milan et al. 2000) for an initial two-point assignment. The RH map was constructed with Carthagene software (Schiex and Gaspin 1997; Schiex et al. 2001), using markers publicly available on the IMpRH Server. Linkage groups were established with a

LOD threshold of 6. For each linkage group, a 1000:1 framework map was built under a haploid model, by a stepwise locus adding strategy, by using as a starting point the triplet of markers whose order is the most likely. The automatically built framework was improved to cover larger distances by removing some markers that prevented its extension and trying, when possible, to include genes instead of microsatellites. The different provisional frameworks were checked with a simulated annealing algorithm testing inversion of fragments of the map, and a flips algorithm testing all local permutations in a window of six markers. After validation of the framework map built under the haploid model, the framework was also confirmed under the diploid model. Finally, markers not included in the framework were mapped relative to framework markers to determine their most likely positions. The human reference map was built from data available at UCSC Web site (<http://genome.ucsc.edu/cgi-bin/hgGateway>, June 2002). RH maps were drawn with MapChart 2.0 (Voorrips, 2002).

Two-color fluorescence in situ hybridization. FISH was performed according to the procedure described previously (Yerle et al. 1994). Briefly, 150 ng of each BAG DNA was labeled by incorporation of biotinylated 16-dUTP or digoxigenin 11-dUTP (Boehringer Mannheim, Indianapolis, IN) with random priming. Hybridization signals were detected by using avidin conjugated to Texas Red and were amplified with goat biotinylated anti-avidin antibody followed by a final incubation with avidin conjugated to Texas Red for the biotinylated probes (*GSTA3* and *SSC2B02*). Digoxigenin-labeled probes (*SSC2B02*, *FLJ10775*, and *BAG2*) were detected with sheep anti-digoxigenin antibody conjugated to FITC. Analyses of the relative position of the fluorescent spots were carried out on at least 20 metaphases by using the Cytovision analysis system (Applied Imaging Corporation, Santa Clara, Calif.).

Results

To develop porcine markers for selected genes, different approaches were followed depending on available porcine sequences. Primers were developed in two consecutive exons framing an intron, within 5' or 3' UTR sequence or within an exon in those regions, which are only moderately conserved between pig and human. Markers were developed with a variable efficiency depending on the location of primers chosen in the gene sequence. Out of 14 primer pairs selected framing one intron, 11 successfully amplified one fragment (79%). Using the 8 primer pairs designed in 3'UTR, 5 markers were

successfully developed (63%). The only pair located in 5' UTR amplified the expected fragment. Three out of the 5 primer pairs selected into an exon were efficiently used (60%). Out of 28 tested markers, 20 were available for the subsequent mapping of the corresponding gene (Table 1). As part of building the BAC contigs along the candidate region, five BACs containing known genes were subcloned (Barbosa et al. in preparation). One microsatellite marker was developed from each of these BAC.

For all the analyzed markers, an average retention frequency of 35% was observed, ranging from 22% (*CD2AP* and *DKFZP566C243*) to 54% (*HKE4* and *SSC2B02*). Genes were assigned by using IMPRH Server (<http://imprh.toulouse.inra.fr>; Milan et al. 2000). Among the developed markers, all but *FLJ13159* were assigned to SSC 7. *FLJ13159* was assigned to SSC 1, with significant linkage to *Sw1653* (LOD 11.42) and *Sw2130* (LOD 11.05). Vectors obtained in the QTL region for the 24 new genes were analyzed together with the 162 markers publicly available for SSC 7 (including 22 genes). We assigned our new markers to two different linkage groups containing a total of 112 markers (including 22 new genes) and 49 markers (including 2 new genes, *MCM3* and *HELO1*), by using a LOD threshold of 6. A 1000:1 framework map was built with Carthagene software (Schiex et al. 2001) for the first linkage group by using a stepwise locus adding strategy under the haploid model. The resulting framework was subsequently extended by including markers from the second linkage group in the analysis. This allowed us to add *GSTA3* to the final framework. This framework map covers 1528 cR_{7.000} (calculated under the diploid model) and includes 16 of the 24 new genes mapped on SSC 7 (Fig. 1). The 8 additional genes (*DAXX*, *DEF6*, *PTK7*, *DKFZP566C243*, *CD2AP*, *BMP5*, *MCM3*, and *HELO1*) were mapped at their most likely location relative to markers of the framework.

To compare the order of genes between the two species, we obtained the location of these genes in the human genome from the UCSC Web site (<http://genome.ucsc.edu/cgi-bin/hgGateway>, June 2002). Complete conservation was observed for the whole region except for three genes, *FLJ10775*, *BMP5*, and *BAG2*, which are located distal to *GSTA3* on the human map and which are located between *HKE4* and *RAB2L* on the porcine framework map, around 20 Mb upstream compared with the human location (Fig. 1).

The non-annotated EST *SSC2B02* (Jorgensen et al. 1997) was mapped at 3 cR_{7.000} from *BMP5* gene. We tried to identify the corresponding gene, using BLASTN software (version 2.2.1) against the latest

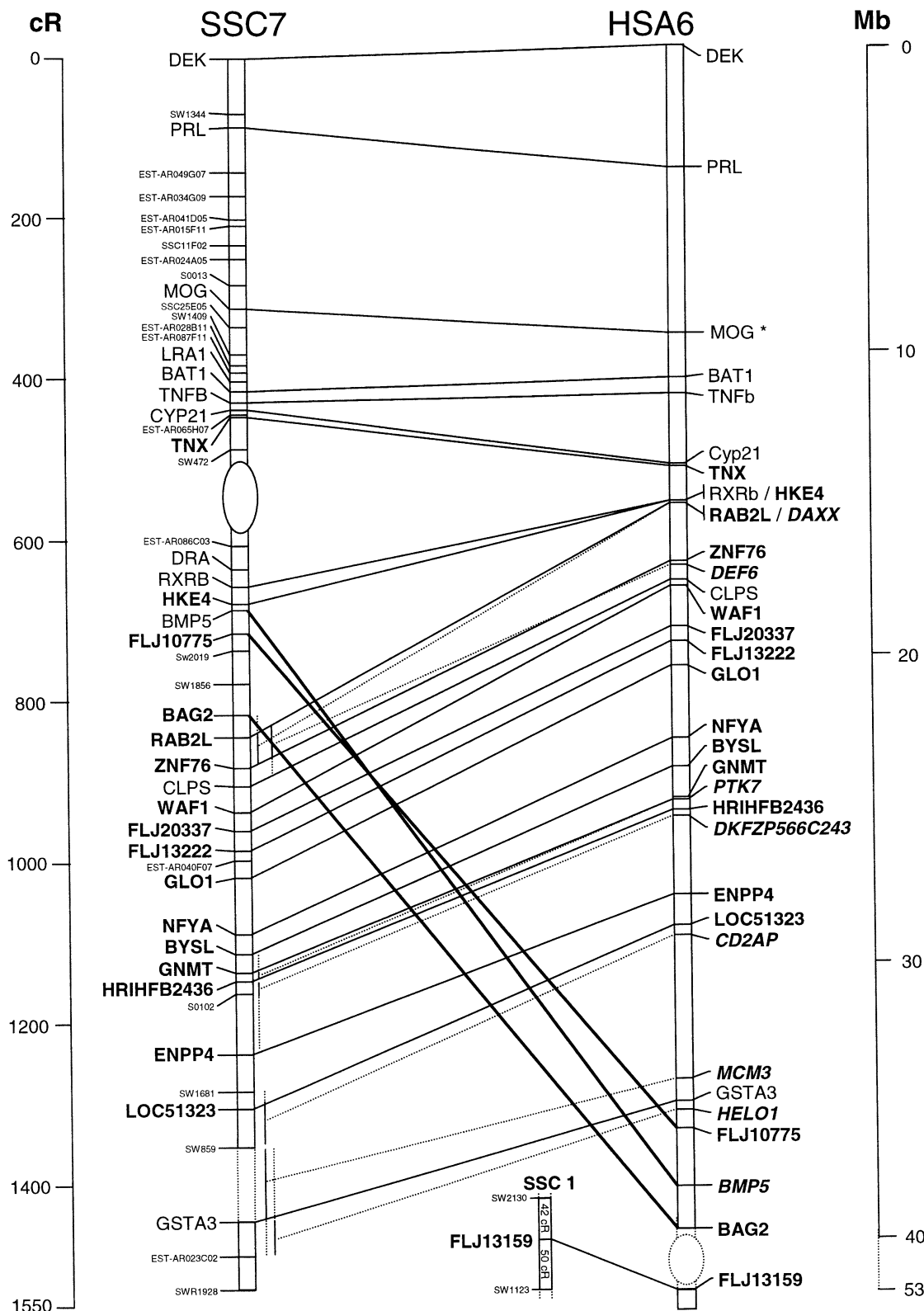


Fig. 1. Detailed comparative map between HSA 6p23-q12 physical map and SSC 7p11-q14 radiation hybrid map. The human physical map has been built with UCSC June 2002 database (<http://genome.ucsc.edu/cgi-bin/hgGateway>). Our markers are in bold and the markers not included in the porcine framework are indicated in italics on the human map. The most likely position of the markers not included in the framework map is represented by a full line, while the alternate position is represented by a dotted line. Centromeres are represented by circles. *: MOG has been placed by using the NCBI build 29 information.

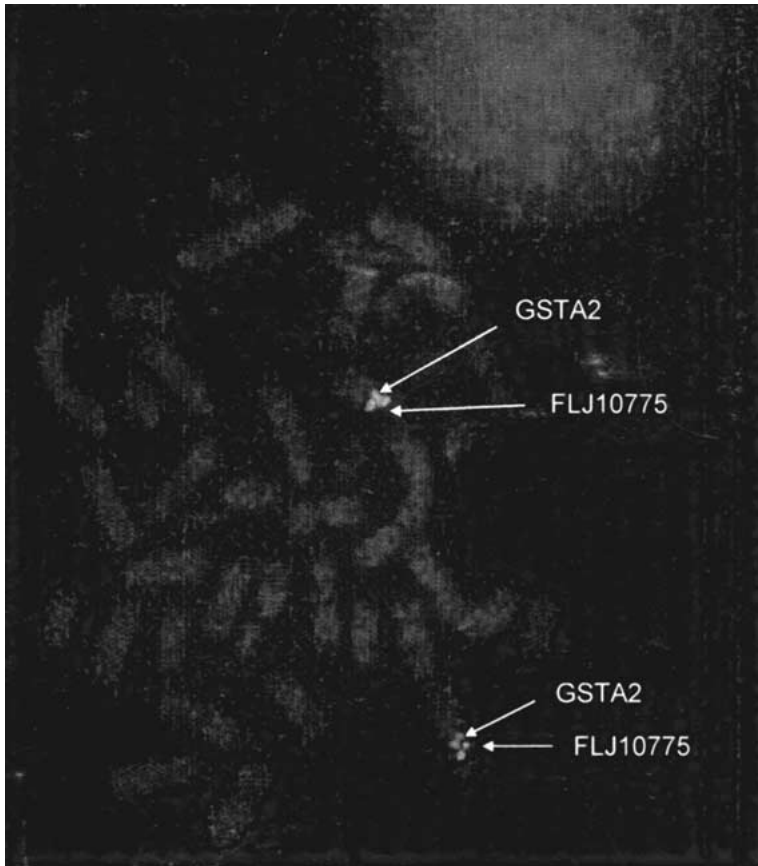


Fig. 2. Two-color fluorescence in situ hybridization with FLJ10775 (in green) and GSTA3 (in red) cohybridized on a porcine metaphase (counter stained in blue). The picture clearly demonstrates that FLJ10775 is situated above GSTA3. A color version of this figure is provided on the cover of this issue.

release of the nt section of GenBank. Significant homology (89% on 428bp; $p = 10^{-129}$) was found to the human *BMP5* gene itself (XM_004361). In order to confirm the location of *BMP5*, *FLJ10775*, and *BAG2* in the pig genome by a second, independent technique, we mapped these genes by two-color Fluorescence In Situ Hybridization (FISH). BAC clones containing these three genes were selected from the INRA BAC library (Rogel-Gaillard et al. 1999). A BAC clone was also screened for *GSTA3* (Tosser-Klopp et al. unpublished), which in the human genome is the first available marker upstream from the three shifted genes. Three double-color FISH experiments were carried out, with *GSTA3* and a second gene-specific probe simultaneously. Analyses of the position of the fluorescent spots indicated that *BMP5*, *FLJ10775*, and *BAG2* are situated on SSC 7q1.2, while *GSTA3* is located on SSC 7q1.4 (Fig. 2). The two BACs containing *BMP5* and *BAG2* were also tested in two-color FISH. A yellow signal was revealed, indicating that these genes have the same cytogenetic position and could not be differentiated by FISH.

The location of the segment containing *BMP5*, *FLJ10775*, and *BAG2* differs between humans and pigs. The map built on IMpRH panel suggests that

these three genes are not in the same order in the two species. We calculated the likelihood of the six possible orders for these three genes. Difference of likelihood with the most likely order ranging from 17.29 to 37.48 was obtained, demonstrating that gene order as determined on the IMpRH panel is highly likely. Even though this order is thus strongly supported, we decided to analyze this region on the newly available 12,000 rad panel IMNpRH2 (Yerle et al. 2002). On this panel we analyzed 10 markers and genes available in this region. We observed an average retention fraction of 42% for these markers, ranging from 33 (*Sw2019*) to 55% (*HKE4*). However, owing to the high-resolution power of the IMNpRH2 panel and the limited number of markers analyzed, it was not possible to build a framework map covering the region by using only data produced on the IMNpRH2 panel. The comprehensive map built with IMNpRH2 data presents the same order as the framework map built by using the IMpRH panel. Moreover, when we recalculated the likelihood for the six possible orders of *BMP5*, *FLJ10775*, and *BAG2* on IMNpRH2, the difference of likelihood with the second best order was of 4.74. On the two panels, the difference of likelihood between the most likely order and the order observed in the human genome

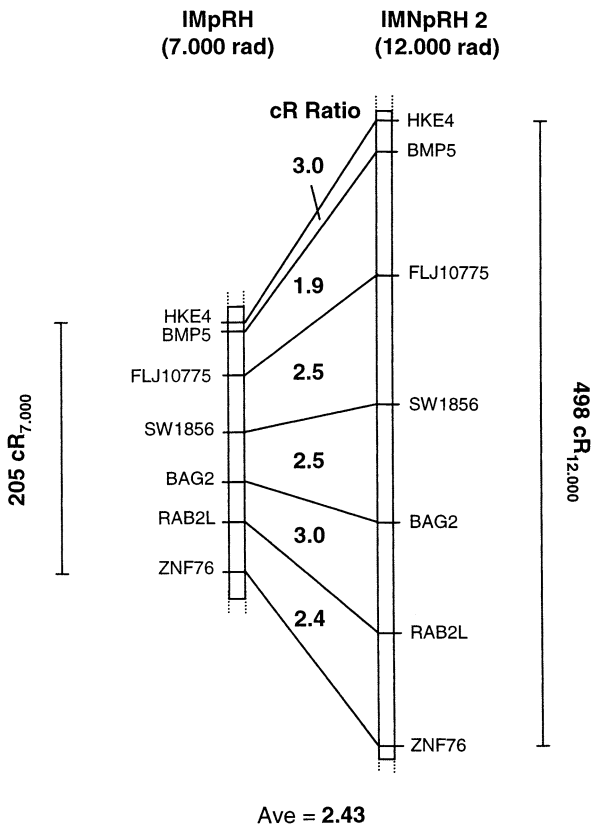


Fig. 3. Representation of the difference of resolution between IMpRH and IMNpRH2 panels.

(*FLJ10775*–*BMP5*–*BAG2*) is 17.29 and 10.9 respectively. These results clearly indicate that the order proposed in the human genome assembly is different from the order observed on pig RH panels. Comparison of distances observed between genes or markers among the two panels revealed that in the studied region, which covers approximately 5 Mb, the IMNpRH2 12.000 rads displays on average a 2.43-fold higher resolution (from 1.9 to 3) than the IMpRH 7000 rad panel (Fig. 3).

Discussion

Numerous QTL influencing traits such as growth, back fat thickness, and carcass composition have been detected on SSC 7 (see Bidanel et al. 2001; de Koning et al. 2001; Malek et al., 2001; Milan et al. 2002 for recent results). A detailed comparative map analysis of this QTL region was thus required to facilitate identification of the responsible gene(s). Previously, we compared the order of genes located on SSC 7p and HSA 6p (Genet et al. 2001). We observed an overall conservation of gene order in this region. In the present study, we compared the order of genes located on HSA 6p, which are localized on SSC 7q11–q14. In the human genome region

HSA6p11.2–q12–13, we selected 28 regularly spaced genes. The selection of genes was greatly facilitated by the use of ICCARE database that displays all human genes for which at least one porcine EST has been sequenced, sorted by their location on the human genome.

In addition to genes mapped in this study, a 162 vectors were publicly available for SSC 7 (including 22 genes spread over the whole chromosome). To handle this data set, it appeared that RMAP3.0 (Lange et al. 1995) was not sufficiently powerful. We used Carthagene software v0.9 (Schiex et al. 2001), which permits analysis of RH data under a haploid or diploid model. Using both flips and simulated annealing algorithms, we tested the framework map automatically constructed by Carthagene. The map was manually improved to identify a confirmed framework. In comparison with previous RH maps available for this region (Hawken et al. 1999; Genet et al. 2001), this study provides the first framework map covering the whole QTL region.

All genes located on HSA6p for which we successfully developed a marker were assigned to SSC 7. *FLJ13159* mapped to HSA6q12–q13 was the most proximal gene on HSA6q for which a marker was successfully developed. In the pig, this gene was assigned to SSC 1, which confirms previous results obtained by FISH painting (Goureau et al. 1996) or heterologous FISH mapping of human YACs (Goureau et al. 2000). To compare gene order between the human and pig genomes, we used physical maps available since June 2002 on UCSC Web site. For MOG gene, we used the build29 NCBI assembly, which presents the region from DEK to BAG2 in a single finished contig (NT_007592.9).

Gene order observed on the IMpRH porcine map is fully consistent with the human order except for a fragment of three genes *FLJ10775*, *BMP5*, and *BAG2*, which is found in pig 20 Mb above the expected location, calculated according to its location in the human genome (this will be discussed below). Overall, the studied region covers 40 Mb of the human genome. Supposing that the porcine orthologous region has a similar size in Mb, and considering that the IMpRH map covers 1528 cR_{7,000}, we observed a ratio of 26 kb/cR_{7,000} in this region. This is an intermediate value between the 14.5 kb/cR_{7,000} observed on *SLA* region by Genet et al. (2001), and the 53 kb/cR_{7,000} proposed for the whole SSC 7 (Hawken et al. 1999). Moreover, the relative distances between genes in the pig and human genomes are well conserved on the whole studied region (Fig. 1), except for two adjacent fragments: the *CYP21*–*HKE4* region and the *HKE4*–*RAB2L* interval framing the shifted fragment *FLJ10775*–*BAG2*. The

chromosomal fragment containing *CYP21* and *HKE4* genes is enlarged in the pig genome by the presence of the centromere of SSC 7. The second modified region identified in our study is the region containing the three genes *FLJ10775*, *BMP5*, and *BAG2*. From the distances observed on the IMpRH and UCSC maps, we consider the boundaries of the shifted chromosomal region as relatively well defined by *FLJ10775* and *BAG2* with a possible extension of up to 800 kb under *BAG2*. From these results, in the studied porcine QTL region, we consider as unlikely the presence of genes found in the human genome outside of HSA6p.

The *FLJ10775*–*BAG2* region is particularly important as it contains two microsatellites (*Sw2019* and *Sw1856*) in pigs, which flank the most likely QTL location in the INRA QTL experiment (Bidanel et al. 2001; Milan et al. 2002). Owing to the location of the shifted fragment in the QTL region, we verified the modification of gene order in this region by two independent analyses. We verified by FISH that these three genes are located in pigs on 7q12 above *GSTA3*, mapped at 7q14, whereas they are found 1–4 Mb below *GSTA3* in the human genome. In addition to the shift of this fragment, their mapping on IMpRH allowed us to identify a modification of gene order in this segment. On the IMpRH panel, the

order *BMP5*–*FLJ10775*–*BAG2* presents a difference of likelihood of 17.29 relatively to the order *FLJ10775*–*BMP5*–*BAG2* observed in the human genome. We took advantage of the availability of the newly developed IMNpRH2 12000 rad panel (Yerle et al. 2002) to confirm the modification of gene order. This study is one of the first performed with the IMNpRH2 panel. We observed an increase of resolution of 2.43-fold between the 7,000 and 12,000 rad panels. Considering a resolution of 26 kb/cR_{7,000} on IMpRH panel, we estimate the resolution on the IMNpRH2 panel at 10.7 kb/cR_{12,000}, which is very similar to the value of 12.5 kb/cR_{12,000} observed in the panel characterization by Yerle et al. (2002) in the RN region, on SSC 15.

The two chromosomal fragments *CYP21*–*HKE4* and *HKE4*–*RAB2L* that are not completely conserved (either in size or gene order) between the pig and human genomes are adjacent. Comparative analysis of the region *HKE4*–*RAB2L* in the pig, human, and mouse genomes shows that it is highly rearranged (Fig. 4). In the mouse genome, fragments corresponding to this region are located on three different chromosomes (17, 9, and 1). Moreover, the *BMP5*–*BAG2* segment is broken, *BMP5*–*FLJ10775* being located on MMU9, whereas *BAG2* maps to MMU1. In human and mouse, *GSTA3* and *FLJ10775*

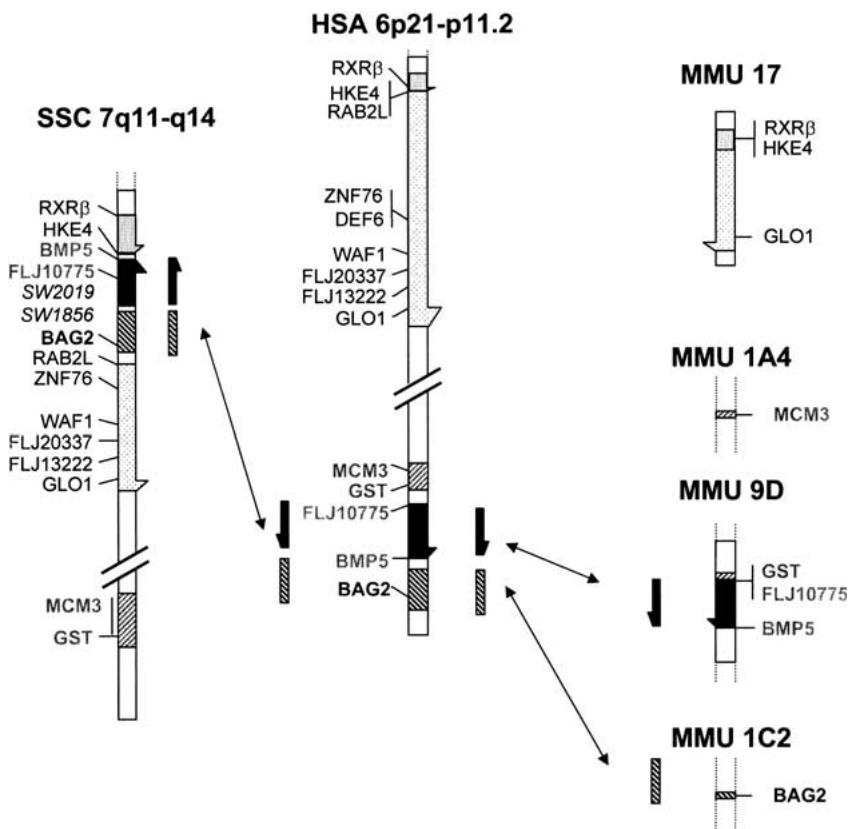


Fig. 4. Evidence of a highly rearranged region in pig, mice, and human species. The pig representation is based on our IMpRH_{7,000} framework map, while the human map has been drawn with the UCSC august 2001 database (<http://genome.ucsc.edu/cgi-bin/hgGateway>). For the mice, we used data from the Jackson laboratory genetic database (<http://www.informatics.jax.org/>) when available. When it was not available, we used the human sequence with the blast function of ensembl genome browser web site (http://www.ensembl.org/Mus_musculus/blastview, Mouse v 4.1.1 31/01/2002).

are physically very close, which is a strong argument for a specific gene order in the pig lineage, which differs from the one observed in rodents and primates.

We could not exclude that more subtle rearrangements, undetected in the present study, have occurred in this region, extending from *CYP21* to *ZNF76*. In addition, this region contains the *SLA* and the SSC 7 centromere. It is known, for instance, that gene duplications have occurred in this region, as evidenced by a detailed comparative analysis of the *HLA* and *SLA* complex (Chardon et al. 1999). A complete physical map of this region is under construction (Barbosa et al. in preparation), but a sequencing of a BAC contig covering the entire region will probably be required for a complete comparative analysis of the organization of the pig and human genomes. The map presented here will provide a valuable framework for anchoring the physical map.

In the context of QTL mapping and positional candidate gene approaches, identification of a shifted chromosomal segment of around 3.7 Mb is very important. Genes found in this segment, which were previously considered as out of the most likely region, could be responsible for the observed QTL effect. If no obvious candidates are found in the shifted segment, we may not totally exclude that *BMP5* itself can be involved, at least in part, in the observed phenotype, since it influences the skeleton development and is required for normal development of several soft tissues (King et al. 1994). Moreover, *CLPS*, which was previously mapped by Genet et al. (2001), is close to the shifted fragment. It is also a possible candidate, as a recent study describes its effect on body weight regulation by using knockout mice (D'Agostino et al. 2002). *HELO1* was another possible candidate, because it is involved in elongation of polyunsaturated fatty acids, which are important membrane components. A study in *Caenorhabditis elegans* recently revealed that an alteration of this pathway induces growth defects (Watts and Browse 2002). Nevertheless, *HELO1* is the first gene we mapped outside of the shifted fragment. It remains, thus, outside of the QTL region.

Studies of *BMP5* and *CLPS* expressions in pigs should be carried out to investigate their potential implication. A search for variants in Meishan and Large White animals will also be required to determine whether those genes should be considered as strong positional candidates for a QTL observed on SSC7, influencing numerous traits including growth and fat deposition in pigs, and composition of pork carcasses.

References

1. Amarante MR, Yang YP, Kata SR, Lopes CR, Womack JE (2000) RH maps of bovine chromosomes 15 and 29: conservation of human chromosomes 11 and 5. *Mamm Genome* 11, 364–368
2. Bidanel JP, Milan D, Iannuccelli N, Amigues Y, Boscher MY et al. (2001) Detection of quantitative trait loci for growth and fatness in pigs. *Genet Sel Evol* 33, 289–309
3. Chardon P, Renard C, Vaiman M (1999) The major histocompatibility complex in swine. *Immunol Rev* 167, 179–192
4. Chardon P, Renard C, Rogel-Gaillard C, Vaiman M (2000) The porcine Major Histocompatibility Complex and related paralogous regions: a review. *Genet Sel Evol* 32, 109–128
5. Cox DR, Burmeister M, Price ER, Kim S, Myers RM (1990) Radiation hybrid mapping: a somatic cell genetic method for constructing high-resolution maps of mammalian chromosomes. *Science* 250, 245–250
6. D'Agostino D, Cordle RA, Kullman J, Erlanson-Albertsson C, Muglia LJ et al. (2002) Decreased postnatal survival and altered body weight regulation in procolipase-deficient mice. *J Biol Chem* 277, 7170–7177
7. de Koning DJ, Janss LL, Rattink AP, van Oers PA, de Vries BJ et al. (1999) Detection of quantitative trait loci for backfat thickness and intramuscular fat content in pigs (*Sus scrofa*). *Genetics* 152, 1679–1690
8. de Koning DJ, Harlizius B, Rattink AP, Groenen MA, Brascamp EW et al. (2001) Detection and characterization of quantitative trait loci for meat quality traits in pigs. *J Anim Sci* 79, 2812–2819
9. Fahrenkrug SC, Freking BA, Rohrer GA, Smith TPL, Casas E (2000) Design and use of two pooled tissue normalized cDNA libraries for EST discovery in swine. Unpublished
10. Genet C, Renard C, Cabau C, Rogel-Gaillard C, Gellin J et al. (2001) In the QTL region surrounding porcine MHC, gene order is conserved with human genome. *Mamm Genome* 12, 246–249
11. Goureau A, Yerle M, Schmitz A, Riquet J, Milan D et al. (1996) Human and porcine correspondence of chromosome segments using bidirectional chromosome painting. *Genomics* 36, 252–262
12. Goureau A, Vignoles M, Pinton P, Gellin J, Yerle M (2000) Improvement of comparative map between porcine chromosomes 1 and 7 and human chromosomes 6, 14, and 15 by using human YACs. *Mamm Genome* 11, 796–799
13. Gu Z, Womack JE, Kirkpatrick BW (1999) A radiation hybrid map of bovine Chromosome 7 and comparative mapping with human Chromosome 19 p arm. *Mamm Genome* 10, 1112–1114.
14. Hawken RJ, Murtaugh J, Flickinger GH, Yerle M, Robic A et al. (1999) A first-generation porcine whole-genome radiation hybrid map. *Mamm Genome* 10, 824–830
15. Jorgensen CB, Wintero AK, Yerle M, Fredholm M (1997) Mapping of 22 expressed sequence tags isolated

from a porcine small intestine cDNA library. *Mamm Genome* 8, 423–427

16. King JA, Marker PC, Seung KJ, Kingsley DM (1994) BMP5 and the molecular, skeletal, and soft-tissue alterations in short ear mice. *Dev Biol* 166, 112–122
17. Lange K, Boehnke M, Cox DR, Lunetta KL (1995) Statistical methods for polyploid radiation hybrid mapping. *Genome Res* 5, 136–150
18. Malek M, Dekkers JC, Lee HK, Baas TJ, Rothschild MF (2001) A molecular genome scan analysis to identify chromosomal regions influencing economic traits in the pig. I. Growth and body composition. *Mamm Genome* 12, 630–636
19. Milan D, Hawken R, Cabau C, Leroux S, Genet C et al. (2000) IMpRH server: an RH mapping server available on the Web. *Bioinformatics* 16, 558–559
20. Milan D, Bidanel JP, Iannuccelli N, Riquet J, Amigues Y et al (2002) Detection of quantitative trait loci for carcass composition traits in pigs. *Genet Sel Evol*, in press
21. Rink A, Santschi EM, Beattie CW (2002) Normalized cDNA Libraries from a porcine model of orthopedic implant associated infection. *Mamm Genome* 13, 198–205
22. Robic A, Seroude V, Jeon JT, Yerle M, Wasungu L et al. (1999) A radiation hybrid map of the RN region in pigs demonstrates conserved gene order compared with the human and mouse genomes. *Mamm Genome* 10, 565–568
23. Rogel-Gaillard C, Bourgeaux N, Billault A, Vaiman M, Chardon P (1999) Construction of a swine BAG library: application to the characterization and mapping of porcine type C endoviral elements. *Cytogenet Cell Genet* 85, 205–211
24. Schiex T, Gaspin C (1997) CARTHAGENE: constructing and joining maximum likelihood genetic maps. *Proc Int Conf Intell Syst Mol Biol* 5, 258–267
25. Schiex T, Chabrier P, Bouchez M, Milan D (2001) Boosting EM for Radiation Hybrid and Genetic Mapping. WABI'2001 (Workshop on Algorithms in Bioinformatics), LNCS 2149.
26. Voorrips RE (2002) MapChart: software for the graphical presentation of linkage maps and QTLs. *J Hered* 93, 77–78
27. Walter MA, Spillett DJ, Thomas P, Weissenbach J, Goodfellow PN (1994) A method for constructing radiation hybrid maps of whole genomes. *Nat Genet* 7, 22–28
28. Watts JL, Browse J (2002) Genetic dissection of polyunsaturated fatty acid synthesis in *Caenorhabditis elegans*. *Proc Natl Acad Sci USA* 99, 5854–5859
29. Yerle M, Goureau A, Gellin J, Le Tissier P, Moran C (1994) Rapid mapping of cosmid clones on pig chromosomes by fluorescence in situ hybridization. *Mamm Genome* 5, 34–37
30. Yerle M, Pinton P, Robic A, Alfonso A, Palvadeau Y et al. (1998) Construction of a whole-genome radiation hybrid panel for high-resolution gene mapping in pigs. *Cytogenet Cell Genet* 82, 182–188
31. Yerle M, Pinton P, Delcros C, Arnal N, Milan D et al (2002) Generation and characterization of a 12,000 rads radiation hybrid panel for fine mapping in pig. *Cytogenet Genome Res* (in press)